



Contents lists available at ScienceDirect

International Journal for Parasitology

journal homepage: www.elsevier.com/locate/ijpara*IrCL1* – The haemoglobinolytic cathepsin L of the hard tick, *Ixodes ricinus*

Zdenek Franta^{a,b}, Daniel Sojka^a, Helena Frantova^{a,b}, Jan Dvorak^{a,e,1}, Martin Horn^c, Jindrich Srba^c, Pavel Talacko^c, Michael Mares^c, Eric Schneider^d, Charles S. Craik^d, James H. McKerrow^e, Conor R. Caffrey^e, Petr Kopacek^{a,*}

^a Institute of Parasitology, Biology Centre of the Academy of Sciences of the Czech Republic, Ceske Budejovice, CZ 37005, Czech Republic^b Faculty of Science, University of South Bohemia, Ceske Budejovice, CZ 37005, Czech Republic^c Institute of Organic Chemistry and Biochemistry, Academy of Sciences of the Czech Republic, Prague, CZ 16610, Czech Republic^d Department of Pharmaceutical Chemistry, University of California San Francisco, San Francisco, CA 94720, USA^e Sandler Center for Drug Discovery, California Institute for Quantitative Biosciences (QB3), University of California San Francisco, San Francisco, CA 94158, USA

ARTICLE INFO

Article history:

Received 10 May 2011

Received in revised form 16 June 2011

Accepted 20 June 2011

Available online xxx

Keywords:

Protease

Cysteine peptidase

Cathepsin

Tick

Ixodes ricinus

Blood meal digestion

Haemoglobin

ABSTRACT

Intracellular proteolysis of ingested blood proteins is a crucial physiological process in ticks. In our model tick, *Ixodes ricinus*, cathepsin L (*IrCL1*) is part of a gut-associated multi-peptidase complex; its endopeptidase activity is important in the initial phase of haemoglobinolysis. We present the functional and biochemical characterisation of this enzyme. We show, by RNA interference (RNAi), that cathepsin L-like activity that peaks during the slow feeding period of females is associated with *IrCL1*. Recombinant *IrCL1* was expressed in bacteria and yeast. Activity profiling with both peptidyl and physiological protein substrates (haemoglobin and albumin) revealed that *IrCL1* is an acidic peptidase with a very low optimum pH (3–4) being unstable above pH 5. This suggests an endo/lysosomal localisation that was confirmed by indirect fluorescence microscopy that immunolocalised *IrCL1* inside the vesicles of digestive gut cells. Cleavage specificity determined by a positional scanning synthetic combinatorial library and inhibition profile indicated that *IrCL1* has the ligand-binding characteristics of the cathepsin L subfamily of cysteine peptidases. A non-redundant proteolytic function was demonstrated when *IrCL1*-silenced ticks had a decreased ability to feed compared with controls. The data suggest that *IrCL1* may be a promising target against ticks and tick-borne pathogens.

© 2011 Published by Elsevier Ltd. on behalf of Australian Society for Parasitology Inc.

1. Introduction

Ticks are worldwide living, blood-feeding, chelicerate arthropods closely related to mites (Subclass: Acari). They are vectors of important pathogens causing severe human and animal diseases (de la Fuente et al., 2008). The hard tick *Ixodes ricinus* is the most important disease vector in Europe, transmitting tick-borne encephalitis virus and the Lyme disease spirochaetes *Borrelia burgdorferi* sensu lato (Nuttall, 1999). Host blood is the ultimate source of energy and nutrients needed for all physiological processes and completion of the tick life cycle (Sonenshine, 1991).

Blood degradation in ticks is an intracellular process localised in the endolysosomal vesicles of gut cells which proceeds at an acidic pH much lower than that of the gut contents (Coons et al., 1986).

* Corresponding author. Address: Institute of Parasitology, Biology Centre ASCR, Branisovska 31, Ceske Budejovice, CZ 37005, Czech Republic. Tel.: +420 387772207; fax: +420 385310388.

E-mail address: kopajz@paru.cas.cz (P. Kopacek).

¹ Present address: Institute of Molecular Genetics, Academy of Sciences of the Czech Republic, Prague, CZ 14220, Czech Republic.

The gut lumen seems to be entirely free of digestive enzymes and serves mainly as a storage organ for the imbibed blood. The bloodmeal uptake by tick digestive cells is executed via fluid phase endocytosis and receptor-mediated endocytosis of clathrin coated pits (Coons et al., 1986). Intracellular digestion of the bloodmeal begins with the fusion of primary lysosomes and endosomes to form secondary lysosomes (digestive vesicles, vacuoles). This process of endocytosis and slow intracellular lysis (termed heterophagy) enables the hard ticks to uptake and digest an enormous amount of blood, exceeding more than 100 times their original body weight (Sonenshine, 1991).

In previous work, we used genetic, biochemical and proteomic tools to describe the suite of digestive peptidases present in the tick gut at a defined feeding stage (semi-engorged females) in *I. ricinus*. We demonstrated that intestinal haemoglobinolysis in this tick relies on Clan CA papain-type cysteine peptidases cathepsins L (*IrCL*), B (*IrCB*) and C (*IrCC*), the Clan CD asparaginyl endopeptidase, legumain (*IrAE*) and the Clan AA aspartic peptidase, cathepsin D (*IrCD*) (Sojka et al., 2008; Horn et al., 2009).

The view that tick digestion relies on a multi-enzyme network or cascade of cysteine and aspartic type peptidases is supported

by reports on individual genes and/or enzymes in different tick species (Renard et al., 2000; Boldbaatar et al., 2006; Sojka et al., 2007; Tsuji et al., 2008; Yamaji et al., 2009; Cruz et al., 2010). Several papain-type cysteine peptidases have been also identified in the midgut transcriptome ('mialome') from the American dog tick, *Dermacentor variabilis* (Anderson et al., 2008) and the midgut proteome from the cattle tick *Rhipicephalus (Boophilus) microplus* (Kongsuwan et al., 2010).

Detailed analysis of the haemoglobinolytic pathway in the *I. ricinus* gut demonstrated that the process is initiated by cleavage of large fragments from haemoglobin by cathepsins D, L and legumain. This is then followed by the activity of cathepsin B, the most abundant peptidase in the cascade. The digestion is completed by the amino- and carboxy-dipeptidase activities of cathepsin C and cathepsin B, respectively (Horn et al., 2009; Franta et al., 2010).

The available tick expressed sequence tag (EST) databases (<http://www.ncbi.nlm.nih.gov/>) and genome-wide dataset of the closely related species *Ixodes scapularis* (<http://iscapularis.vectorbase.org/>) indicate that ticks possess several genes encoding cathepsin L-related peptidases. Accordingly, the main task of this work was to understand whether the previously described cathepsin L (*IrCL1*) gene (GenBank Accession No. EF428205) (Sojka et al., 2008) was responsible for the activity detected in the gut homogenates of semi-engorged females (Horn et al., 2009; Franta et al., 2010). To address this hypothesis, we expressed the recombinant *IrCL1* in *Escherichia coli* and *Pichia pastoris*, and performed a series of enzyme characterisations (optimum pH, stability, substrate/inhibitor specificity). We then compared these properties with those of the native enzyme(s) in tick gut homogenates. Direct evidence of the functional link between the *IrCL1* gene and the corresponding activity was provided by RNA interference (RNAi) which revealed that *IrCL1* is a non-redundant component of the adult female digestive machinery during the slow-feeding period. This result promotes *IrCL1* as a promising candidate antigen for the development of novel anti-tick vaccines targeting the parasite digestive system.

2. Materials and methods

2.1. Experimental animals and tissue dissection

Ixodes ricinus ticks were collected by flagging in woodlands around Ceske Budejovice, Czech Republic. Adult females were allowed to feed naturally on laboratory guinea pigs until full engorgement (days 7–8) or removed forcibly using forceps after a specific time of feeding (days 2, 4, 6 post-attachment). Gut tissues from unfed and fed females were dissected under a binocular microscope and the excess of blood was washed in PBS. Cleaned gut tissues were pooled and used for RNA isolation or gut tissue extraction. All animals were treated in accordance with the Animal Protection Law of the Czech Republic No. 246/1992 sb., ethics approval number 137/2008.

2.2. Isolation of total RNA, cDNA preparation and gut tissue extraction

RNA isolation and cDNA synthesis were executed as described previously (Franta et al., 2010). Briefly, total RNA was isolated using a NucleoSpin® RNA II kit (Macherey-Nagel, Germany) and stored at –80 °C prior to cDNA synthesis. Single-stranded cDNA was reverse-transcribed from 0.5 µg of total RNA using the Transcriptor High Fidelity cDNA Synthesis kit (Roche, Germany). Gut tissue extract was prepared and used for activity assays or western blotting analyses as described previously (Horn et al., 2009).

2.3. Expression, refolding, purification of recombinant *IrCL1* in *E. coli* and production of polyclonal antibodies

A 964 bp long fragment encoding *IrCL1* pro-enzyme (Sojka et al., 2008) was amplified from the gut cDNA of semi-engorged *I. ricinus* females using specific forward 5'-CACCGTCAGCTACCAGGAAG-3' (adaptor used for cloning into a pET100 vector is underlined) and reverse 5'-GGGGTCAAAGTGCAGATACGG-3' primers. PCR product was cloned into the *E. coli* expression vector pET100/D-TOPO® (Invitrogen) and verified by DNA sequencing. Recombinant *IrCL1* (termed as *IrCL1_{Ec}*) pro-enzyme was produced in *E. coli* with a N-terminal 6× His tag and purified from inclusion bodies using Co²⁺ chelating chromatography under denaturing conditions as described previously (Sojka et al., 2007). *IrCL1* pro-enzyme denaturated in 8 M urea was reduced (1 h at 26 °C) in 50 mM reduced glutathione and incubated (4 days at 4 °C) at a concentration of 10 µg/ml in the re-folding cocktail: 50 mM Tris pH 8.0, 30% glycerol, 0.05% polyethylene glycol 1500, and 5 mM/0.5 mM reduced/oxidised glutathione. Refolded protein was purified by fast protein liquid chromatography (FPLC) using an ÄKTA-FPLC™ system and a Mono Q HR 5/5 column (GE Healthcare Bio-Sciences, Sweden) equilibrated with 50 mM Tris pH 8.0, 10% glycerol and 0.05% 2-mercapthoethanol, and eluted using a linear gradient of 0–0.5 M NaCl. The resulting *IrCL1_{Ec}* was activated in 50 mM Na-acetate pH 4.0, 1 mM DTT for 2–3 h at 26 °C, and was subsequently reversibly inhibited by addition of 5 mM S-methylmethanethiosulphonate (S-MTS) to prevent *IrCL1_{Ec}* autodegradation. The purification and activation process was monitored by hydrolysis of Z-Phe-Arg-AMC substrate (benzyloxycarbonyl-phenylalanylarginine-7-amido-4-methylcoumarin, Bachem, Switzerland; see Section 2.5) and SDS-PAGE.

Purified enzyme was used to immunise a rabbit to obtain specific polyclonal antibodies as described previously (Kopacek et al., 2003). In order to increase the specificity of the *IrCL1* detection and to reduce the background fluorescence of the gut semi-thin sections visualised by indirect fluorescence microscopy, the rabbit antibodies (Ra×*IrCL1*) were further processed and purified by affinity chromatography using the *IrCL1_{Ec}* coupled to the CNBr-activated sepharose according to the previously described method (Franta et al., 2010).

2.4. Expression and purification of active *IrCL1* in *P. pastoris*

Specific primers: forward 5'-TCTCTCGAGAAAAGAGTCAGCTACCAGGAAG-3' containing an *Xho* I restriction site (underlined) and a *Kex2* peptidase cleavage site and reverse 5'-ATTCTAGATTACA CAAGAGGTATGC-3' (*Xba* I restriction site is underlined) were used for PCR amplification of *IrCL1* pro-enzyme from tick gut cDNA. The PCR product was ligated into a pPICZαB vector (Invitrogen) and verified by DNA sequencing. *IrCL1* was expressed in *P. pastoris* X33 strain using the procedure described previously (Caffrey et al., 2002). The yeast medium containing recombinant *IrCL1* pro-enzyme was centrifuged at 3,000g for 20 min. Supernatant was filtered (0.45 µm), lyophilised, resuspended in water (to 10% of the original volume) and desalted on a Sephadex G25 column equilibrated with water. *IrCL1* was activated in 50 mM Na-acetate pH 4.0, 1 mM DTT for 15–30 min at 26 °C, and subsequently reversibly inhibited by the addition of 5 mM S-MTS to prevent *IrCL1* autodegradation. *IrCL1* (further referred to as *IrCL1_{Pp}*) was purified by ÄKTA-FPLC™ system using a Mono S HR 5/5 column (GE Healthcare Bio-Sciences) equilibrated with 20 mM Na-acetate buffer pH 4.0 and eluted using a linear gradient of 0–1 M NaCl. The purification and activation process was monitored by hydrolysis of Z-Phe-Arg-AMC substrate (see Section 2.5) and SDS-PAGE.

Table 1
Inhibition sensitivity of recombinant *Ixodes ricinus* cathepsin L (*IrCL1*) by protease inhibitors.

Inhibitor ^a	Specificity/target protease	Inhibitor concentration	Inhibition [%] ^b
E-64	Cysteine proteases ^c	1 μ M	100 \pm 1
Leupeptin	Serine and cysteine proteases ^d	1 μ M	99 \pm 2
Z-Phe-Phe-DMK ^j	Cysteine proteases of cathepsin L type ^e	1 μ M	94 \pm 4
CA-074	Cysteine proteases of cathepsin B type ^f	1 μ M	29 \pm 6
Pepstatin	Aspartic proteases ^g	5 μ M	5 \pm 2
Pefabloc	Serine proteases ^h	0.1 mM	3 \pm 3
EDTA	Metalloproteases ⁱ	1 mM	1 \pm 3

^a Recombinant activated *IrCL1* expressed in *Pichia pastoris* was pre-incubated with the given inhibitor and remaining activity was measured in a kinetic assay with the fluorogenic substrate Z-Phe-Arg-AMC (benzyloxycarbonyl-phenylalanylarginine-7-amido-4-methylcoumarin).

^b Mean values \pm S.D. are expressed as the percentage inhibition compared with the uninhibited control.

^c Barrett et al. (1982).

^d Aoyagi et al. (1969).

^e Caffrey and Ruppel (1997).

^f Murata et al. (1991).

^g Knight and Barrett (1976).

^h James (1978).

ⁱ Auld (1988).

^j Benzyloxycarbonyl-phenylalanylphenylalanine-diazomethyl ketone.

2.5. Cathepsin L activity assays

Cathepsin L activity was measured using Z-Phe-Arg-AMC substrate. Recombinant *IrCL1* (10 ng) or tick gut extract (150 ng) was pre-incubated for 15 min at room temperature in citrate-phosphate-buffer (CPS) pH 2.5–7.0, and 0.2 M glycine/NaOH buffer (glycine buffer), pH 8.0 which contain 100 mM NaCl and 4 mM DTT in final volume of 100 μ l. The reaction was started by adding 100 μ l of the same buffer with 40 μ M of Z-Phe-Arg-AMC substrate. The production of free AMC was continuously measured at excitation and emission wavelengths set to 360 and 465 nm, respectively, in a Labsystems Fluoroskan II fluorescent plate reader (Thermo Electron Corporation, USA). For activity assays in the presence of peptidase inhibitors, an aliquot of *IrCL1*_{Ec} or *IrCL1*_{Pp} was pre-incubated (15 min at room temperature) in CPS buffer pH 4.0 containing 100 mM NaCl and 4 mM DTT with inhibitors (Table 1). For the *IrCL1*_{Pp} stability assay, the enzyme was pre-incubated in CPS buffer pH 3–7 and glycine buffer pH 8 for 1, 2, 4 and 24 h at room temperature. The activity assay was then performed as stated above at pH 4.0. Assay of cathepsin L activity in the tick gut extract was measured in the presence of cathepsin B inhibitor 10 μ M CA-074 (Sigma, Germany) to prevent undesired hydrolysis by cathepsin B (Murata et al., 1991). All measurements were performed in triplicate.

2.6. Hydrolysis of protein substrates by *IrCL1*_{Pp}

Five microlitres of BSA or haemoglobin (20 mg/ml) was incubated with 10 μ l (1.5 μ g/ml) of activated *IrCL1*_{Pp} in CPS buffer pH 3.0–7.0 and glycine buffer pH 8.0 containing 4 mM DTT overnight at room temperature in a final volume of 50 μ l. The inhibition of *IrCL1* was assessed using cysteine protease inhibitor 10 μ M E64 (Sigma). The reaction mixture was resolved by electrophoresis using 4–12% NuPAGE Bis–Tris gel in NuPAGE MES SDS Running Buffer (Invitrogen, USA) and stained with Coomassie Brilliant Blue.

2.7. Substrate profiling of *IrCL1*_{Pp} using a positional scanning synthetic combinatorial library (PS-SCL)

Synthesis of the PS-SCL has been described previously (Choe et al., 2006). The assay was performed at pH 4.0, as described previously (Sojka et al., 2007). Release of 7-amino-4-carbamoylmethyl-coumarin (ACC) was measured in a LS50B luminescence spectrometer (Perkin-Elmer, USA) with excitation and emission wavelengths set to 380 and 460 nm, respectively.

2.8. Active-site labelling of *IrCL1*

Active-site labelling was performed as described previously (Horn et al., 2009). Briefly, an aliquot of the gut tissue extract (0.1–1.0 μ g of protein) or purified *IrCL1*_{Ec} or *IrCL1*_{Pp} (0.1–0.5 μ g of protein) was incubated (1 h at 35 $^{\circ}$ C) with 1 μ M of the active-site probe bodipy green-DCG-04 (Greenbaum et al., 2002). The reaction was performed in 50 mM Na-acetate pH 4.0, 2.5 mM DTT. The competitive labelling was performed after pre-incubation (15 min at 35 $^{\circ}$ C) with 1 μ M Z-Phe-Phe-DMK (benzyloxycarbonyl-phenylalanylphenylalanine-diazomethyl ketone) and/or 1 μ M CA-074 (cathepsin B inhibitor). The labelling reaction was stopped by heating at 70 $^{\circ}$ C in reducing Laemmli sample buffer. The reaction mixture was separated by 15% Laemmli-SDS–PAGE and visualised in a Typhoon 8600 Imager (GE Healthcare) using excitation at 532 nm and the filter set to 580 nm (bp 30 nm).

2.9. Localisation of *IrCL1* in the tick gut cells by indirect immunofluorescence

Dissected gut tissue from *I. ricinus* females (6 days post-attachment) was used for preparing semi-thin sections. The fixation of gut tissue, the *IrCL1* localisation and tissue staining were performed as described previously (Franta et al., 2010). Briefly, the semi-thin sections were blocked in 1% BSA, 10% low fat dry milk, 0.3% Tween 20 in PBS for 10 min, and incubated for 3.5 h with affinity-purified *IrCL1*_{Ec} antibodies (160 μ g/ml) in a humid chamber at room temperature. For negative control experiments, the primary antibody incubation was omitted. After washing with 0.3% Tween 20 in PBS the sections were incubated for 2 h with Alexa Fluor 488-conjugated goat anti-rabbit antibody (Invitrogen/Molecular Probes) diluted to 1:500. The slides were next counterstained with DAPI (2.5 μ g/ml; Sigma). Finally, sections were mounted in 2.5% DABCO (1,4-diazabicyclo[2.2.2]octane; Sigma) dissolved in glycerol, examined using the Olympus FV1000 confocal microscope and consequently processed with the Fluoview (FV10-ASW, Version 1.7) software.

2.10. Profiling of *IrCL1* by quantitative real time PCR (qRT-PCR)

Ixodes ricinus cDNAs prepared from guts dissected at the specified feeding time points were diluted 20 times and 2 μ l were used as a template for qRT-PCR in a final volume of 25 μ l. A dual labelled UPL probe and specific forward 5'-AACCACTGGGGTGATGA-3' and reverse 5'-CAAGAGGTATGCTAGCACTGGA-3' primers were de-

signed online (<http://www.universalprobelibrary.com>; Roche). The reaction was carried out in the Rotor-Gene RG3000 PCR machine (Corbett Research, Australia). Quantitative PCR amplification was as follows: initial denaturation at 95 °C for 10 min, then 40 cycles of 95 °C for 15 s and 60 °C for 60 s. The data were analysed using the Pfaffl equation (Pfaffl, 2001) and the gene for elongation factor 1 α (ELF1A) was used as an internal control (Nijhof et al., 2009). All of the reactions were carried out in triplicate. The *IrCL1* mRNA expression levels at individual time points were related to that of unfed ticks.

2.11. RNAi

RNAi silencing was performed as described previously (Buresova et al., 2009; Hajdusek et al., 2009). Briefly, a 403 bp long fragment of *IrCL1* was amplified from *I. ricinus* gut cDNA using specific forward 5'-ATGGGCCCCAGTGTGGATCTGCTGG-3' and reverse 5'-ATTCTAGAGCTCGTACACACCG-3' primers containing *Apal* and *XbaI* restriction sites (underlined) for directional cloning into the pII10 vector (Levashina et al., 2001). Double stranded RNA was synthesised using a MEGAscript T7 transcription kit (Ambion, UK). The volume of 0.5 μ l (3 μ g/ μ l) was injected into the haemocoel of 25 unfed *I. ricinus* females using a micromanipulator (Narishige, Japan). The control group of 25 ticks was injected with the same volume of double-stranded GFP (dsGFP) synthesised under the same conditions from linearised plasmid pII6 (Levashina et al., 2001). After 24 h of rest in a humid chamber, ticks were allowed to feed naturally on guinea pigs. Semi-engorged females fed for 6 days were forcibly removed from the host, weighed and the guts were dissected to test the *IrCL1* knockdown by western blot analyses and enzymatic activity assays.

3. Results

3.1. Expression of *IrCL1* in *E. coli* and preparation of polyclonal antibodies

The recombinant *IrCL1* pro-enzyme expressed in the *E. coli* system as a (His)₆-tagged fusion protein (*IrCL1*_{Ec}) was isolated from inclusion bodies using Co²⁺-chelating chromatography, renatured and subsequently purified by ion-exchange FPLC (Fig. 1, lane 1). The polyclonal antibodies resulting from immunisation of a rabbit (Ra \times *IrCL1*_{Ig}) reacted with the original *IrCL1*_{Ec} antigen on the western blot (Fig. 1, lane 2). The *IrCL1*_{Ec} pro-enzyme was subjected to activation at an acidic pH, which produced a proteolytically active enzyme capable of hydrolysing the fluorogenic substrate Z-Phe-Arg-AMC. Because the recombinant *IrCL1*_{Ec} had limited stability during storage (data not shown), the enzyme was alternatively produced in the yeast *P. pastoris* (denoted *IrCL1*_{Pp}).

3.2. RNAi of *IrCL1* demonstrates the authenticity of the native enzyme and its role in the feeding phenotype

RNAi was accomplished by injection of *IrCL1* dsRNA, and GFP dsRNA for control, into the tick haemocoel. The Ra \times *IrCL1*_{Ig} antibodies recognised two major bands of approximately 40 and 28 kDa in tick gut homogenates from the GFP control group (Fig. 2A, lane 4). By contrast, these bands were significantly reduced in gut homogenates from ticks injected with *IrCL1* dsRNA (Fig. 2A, lane 3). The size of the larger band corresponds to the theoretical molecular mass of the *IrCL1* pro-enzyme, whereas the 28 kDa band most likely reflects the mature form of the activated enzyme (Sojka et al., 2008). Likewise, peptidolytic activity against the Z-Phe-Arg-AMC substrate (in the presence of a CA-074 inhibitor to block the activity of cathepsin B) was diminished by 95%

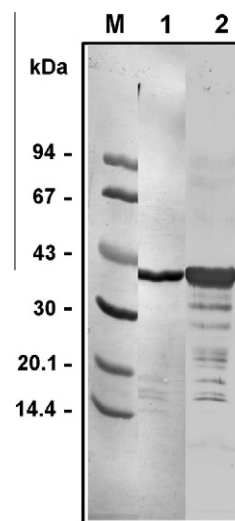


Fig. 1. Preparation of recombinant *Ixodes ricinus* cathepsin L (*IrCL1*) zymogen and specific polyclonal antibodies. Recombinant *IrCL1* zymogen was expressed in *Escherichia coli* as a (His)₆-tagged fusion protein, purified using Co²⁺ chelating chromatography, re-folded and used as antigen to raise antibodies in a rabbit. M, molecular mass standards, protein stained; lane 1, purified recombinant pro-enzyme (pro-) *IrCL1*, protein stained; lane 2, Western blot analysis of purified recombinant pro-*IrCL1* with specific antibodies (Ra \times *IrCL1*_{Ig}).

relative to the control (Fig. 2B). RNAi of *IrCL1* also resulted in decreased weight gain: weights of partially engorged females injected with *IrCL1* dsRNA were decreased by 24% relative to the GFP controls ($P < 0.05$). These data suggest that *IrCL1* plays an important and non-redundant role in the gut-associated multi-enzyme network of ticks.

3.3. *IrCL1* expression during tick feeding on the host

Adult *I. ricinus* females feed on the host for up to 7–8 days. To monitor the change in expression levels of *IrCL1* in the gut tissue during feeding, we set up a series of time points comprising guts from unfed ticks (UF), ticks fed for 2, 4 and 6 days, and fully fed (FF) ticks. The collected females were dissected and analysed either for expression of *IrCL1* mRNA by qRT-PCR (Fig. 3A) or for the amount of the native *IrCL1* in gut homogenates as monitored by western blot analysis (Fig. 3B). The expression profiling by qRT-PCR revealed that the *IrCL1* mRNA level is strongly up-regulated after the second day of feeding and reaches its maximum on the fourth and sixth days post-attachment (Fig. 3A). Interestingly, the mRNA levels of *IrCL1* drop markedly during the period of rapid engorgement (7–8 days post-attachment) and the mRNA expression of *IrCL1* in FF ticks is almost at the same level as in UF ticks. A similar course of expression was also observed for *IrCL1* protein in gut homogenates (Fig. 3B). Only the band of 28 kDa corresponding to the activated enzyme was detected in UF ticks, possibly a remnant from the previous nymphal feeding stage. The significant drop in the amount of protein in the gut homogenates in fully engorged ticks indicates that *IrCL1* is most functional during the slow-feeding period between the days 2 and 6.

3.4. *IrCL1* is localised inside tick gut cells

The general gut structure of the *I. ricinus* semi-engorged female (sixth day post-attachment) is clearly visible in semi-thin sections stained with toluidine blue and monitored under a light microscope (Fig. 4A). Immunolocalisation of the authentic *IrCL1* on semi-thin sections using affinity purified antibodies (Ra \times *IrCL1*_{ACP})

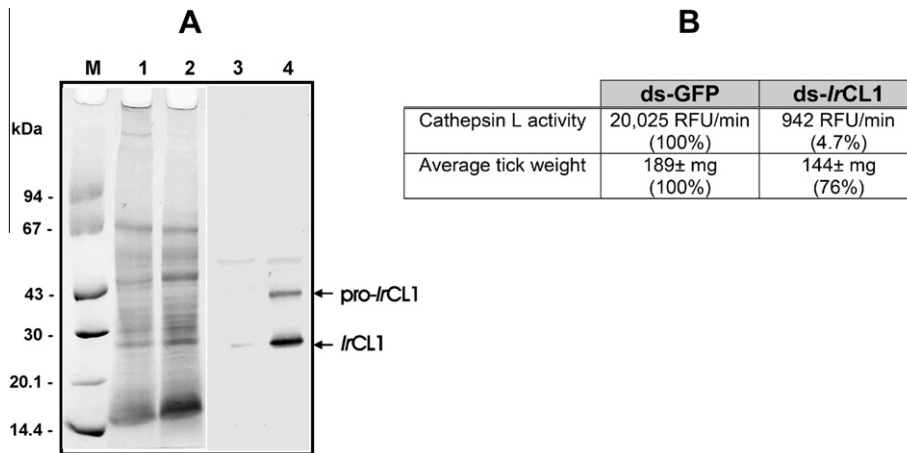


Fig. 2. RNA interference (RNAi) silencing of *Ixodes ricinus* cathepsin L (*IrcL1*). Adult *I. ricinus* females (25 ticks per each group) were injected with *IrcL1* double-stranded RNA (dsRNA) or GFP dsRNA as a control, and allowed to feed naturally on guinea pigs until the day 6. Ticks were then removed and tick weights compared by determination of the average weight of *IrcL1*-silenced and control ticks prior to gut dissection. The guts from both *IrcL1* dsRNA and GFP dsRNA treated groups were homogenised and used for *IrcL1* detection by western blot analysis and enzyme activity measurements. (A) Identification of the authentic *IrcL1* in gut homogenates by RNAi. M, molecular mass standards, protein stained; lanes 1 and 2, SDS-PAGE of tick gut homogenates, protein stained; lanes 3 and 4, Western blot detection of *IrcL1* with specific anti-*IrcL1* antibodies (Ra×*IrcL1*_{ig}). Lanes 1 and 3, *IrcL1*-silenced ticks injected with *IrcL1* dsRNA. Lanes 2 and 4, control ticks injected with GFP dsRNA. The arrows point to the pro-enzyme (pro-*IrcL1*) and an activated form, respectively. (B) The effect of *IrcL1* RNAi silencing on cathepsin L activity and weight-gain. The cathepsin L activity in tick homogenates was measured using a fluorogenic substrate Z-Phe-Arg-AMC (benzyloxycarbonyl-phenylalanylarginine-7-amido-4-methylcoumarin) in the presence of CA-074 inhibitor to shield the activity of cathepsin B. The average weight of *IrcL1*-knockdown ticks was significantly ($P < 0.05$) reduced by approximately 25% compared with the control.

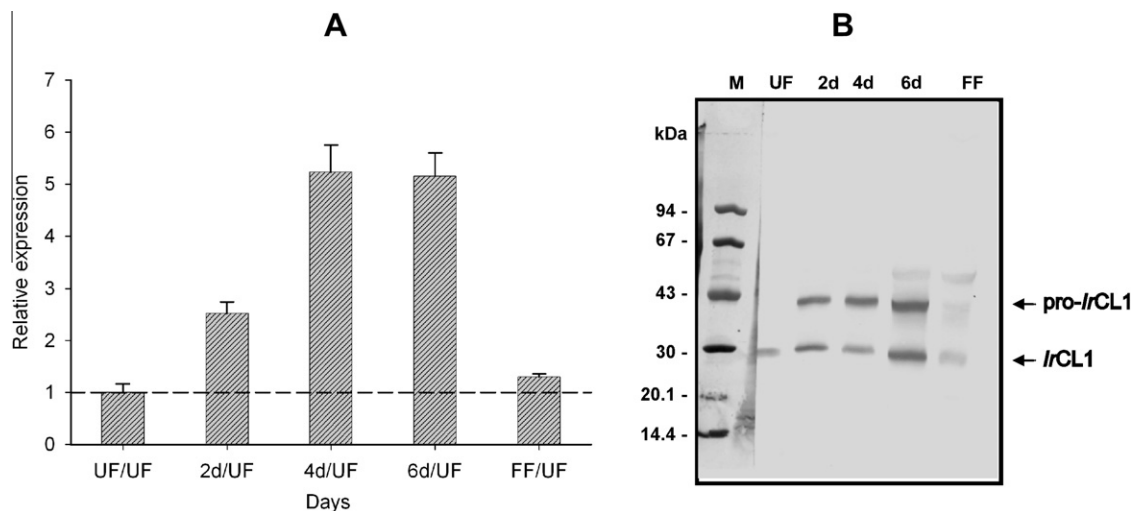


Fig. 3. Dynamics of *Ixodes ricinus* cathepsin L (*IrcL1*) expression during bloodmeal uptake. (A) Expression of *IrcL1* mRNA in the guts dissected from ticks fed for the specified number of days (2d, 4d, 6d) was determined using quantitative real time PCR (qRT-PCR). The levels of *IrcL1* mRNA expression during tick feeding were normalised against the average mRNA level in unfed (UF) ticks. Errors bars depict the S.D. of triplicate measurements. FF, fully fed. (B) Western blot analysis of *IrcL1* in homogenates of guts, dissected at the specified days of feeding, display similar expression profiles at the protein level. M, molecular mass standards, protein stained on the membrane; UF, 0.8 gut/lane; 2d, 0.4 gut/lane; 4d, 0.2 gut/lane; 6d and FF, 0.1 gut/lane. Note that just the activated form of *IrcL1* is present in the unfed tick.

clearly demonstrates the exclusive presence of the enzyme inside the cells growing from the gut wall that are metabolically active (digestive cells; Fig. 4B). No signal was detected in the gut lumen. For the negative control, the primary antibody was omitted and only the Alexa-Fluor® 488 conjugated secondary antibody was applied (Fig. 4C). The presence of *IrcL1* inside the digestive cell compartments further supports this enzyme as a constituent of the endolysosomal tick digestive apparatus.

3.5. Functional expression of recombinant *IrcL1* in the yeast *P. pastoris* and its purification

Because the recombinant *IrcL1*_{EC} had limited stability, the stable recombinant enzyme was alternatively produced in the

yeast *P. pastoris* (denoted *IrcL1*_{pp}). This protein was purified from the expression medium using a multistep protocol leading to the purification of activated enzyme in the final ion-exchange FPLC step (Fig. 5A). We obtained homogenous protein preparation of *IrcL1*_{pp} (Fig. 5A inset); the average yield was 1.5 mg/l of expression media. The activated *IrcL1*_{pp} efficiently cleaved Z-Phe-Arg-AMC (data not shown).

Fig. 5B shows that activated *IrcL1*_{EC}, *IrcL1*_{pp} and the native *IrcL1* can react with the activity-based probe Green-DCG-04 and migrate on SDS-PAGE as single bands (approximately 28, 32 and 30 kDa, respectively). N-terminal sequencing of *IrcL1*_{pp} revealed that the 32 kDa band was generated by cleavage of the Glu¹¹⁵-Asp¹¹⁶ bond. This auto-activation cleavage site is located three amino acid residues upstream of that known for mature human cathepsin L

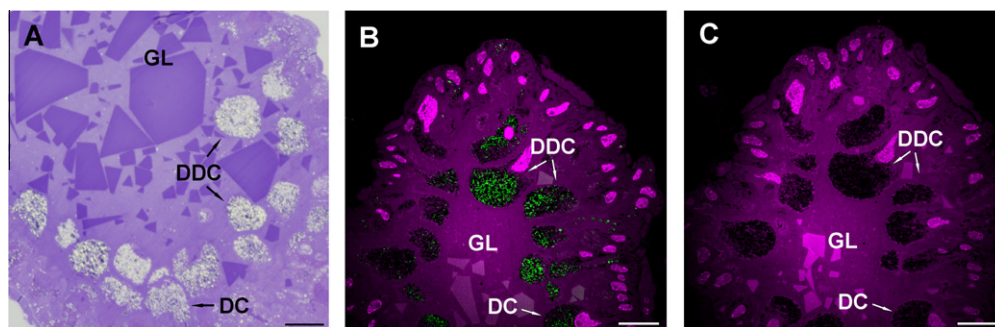


Fig. 4. Localisation of *Ixodes ricinus* cathepsin L (*IrCL1*) in the tick gut by indirect immunofluorescence microscopy. Sections were prepared from adult *I. ricinus* females, which were allowed to feed on guinea pigs for 6 days. Scale bar = 40 μ m. (A) Semi-thin section stained with toluidine blue shows the general structure of tick gut. DC, digestive cells; DDC, detached digestive cells; GL, gut lumen. (B) Semi-thin section labelled with affinity purified rabbit *IrCL1* antibody (Ra \times *IrCL1*_{ACP}). The goat anti-rabbit IgG conjugated with Alexa-Fluor[®] 488 was used as the secondary antibody. Note specific *IrCL1* signal is localised inside tick digestive cells only. (C) Section labelled with secondary antibody only was used as a negative control. Nuclei of cells were counterstained with DAPI (magenta) (B and C). Images are z-stacks of confocal slices (B and C).

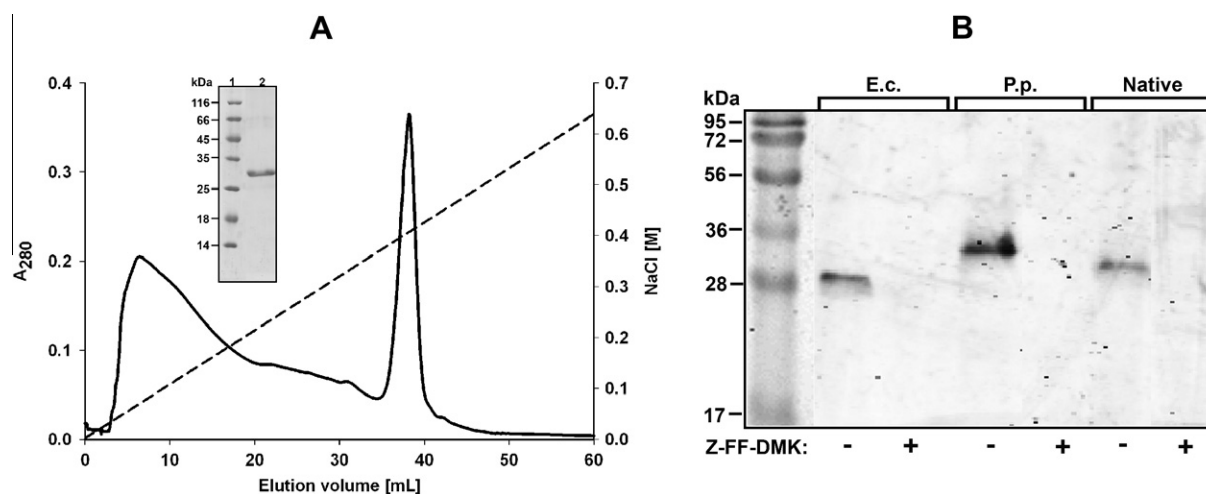


Fig. 5. Isolation of recombinant *Ixodes ricinus* cathepsin L (*IrCL1*) after expression in *Pichia pastoris* and active site labelling. (A) The concentrated and dialysed medium was applied onto a Mono S column and eluted with a gradient of NaCl (dotted line). The fractions with *IrCL1* activity (bar) were assayed with Z-Phe-Arg-AMC (benzyloxycarbonyl-phenylalanylarginine-7-amido-4-methylcoumarin) as a substrate. The inset shows protein-stained SDS-PAGE. Lane 1, molecular mass standards; lane 2, the purified product. (B) Visualisation of activated *IrCL1* by the active site probe bodipy green DCG-04 after SDS-PAGE; *IrCL1* expressed in *Escherichia coli* (E.c.), *Pichia pastoris* (P.p.) and the native *IrCL1* (gut extract). The competitive labelling was performed in the presence of the cathepsin L-specific inhibitor Z-Phe-Phe-DMK (benzyloxycarbonyl-phenylalanylphenylalanine-diazomethyl ketone). Molecular mass standards were protein-stained.

(Supplementary Fig. S1). The size differences can be explained by the degree of glycosylation at two predicted *N*-glycosylation sites (Supplementary Fig. S1) of non-glycosylated *IrCL1*_{Ec}, authentic *IrCL1* and over-glycosylated *IrCL1*_{Pp}.

3.6. *IrCL1* displays a markedly acidic optimum pH

The pH profiles of *IrCL1*_{Ec} and *IrCL1*_{Pp} were determined with Z-Phe-Arg-AMC and compared with that of the native cathepsin L activity in tick gut homogenate (Fig. 6A). All pH profiles had maxima at pH 3.5–4.0. The activity declined steeply at pH 5.0 and the enzyme preparations were ineffective at neutral pH. The enzyme is most stable at the optimum pH but the stability rapidly decreases at higher pH values (Fig. 6B).

3.7. Substrate and inhibitory specificity of *IrCL1*

A PS-SCL (Choe et al., 2006) was used to determine the *IrCL1* cleavage specificity at the substrate P1–P4 positions (Fig. 7). The cleavage map shows that *IrCL1* prefers amino acids with polar side chains at P1. The highest preference was recorded for Arg but other

amino acids could also be accommodated at this position including Gln, Lys, Thr and Glu. In addition, *IrCL1* can well accommodate the hydrophobic residue Met and the non-natural residue norleucine that has a similar unbranched chain structure as Lys. At the P2 subsite position, *IrCL1* prefers bulky aromatic residues (Trp, Phe and Tyr) and branched aliphatic amino acids (Val, Leu and Ile). The P3 position displays rather promiscuous substrate specificity, although Val and Ile are unfavourable. Screening at P4 revealed a low preference for large non-polar residues.

The inhibitory specificity of *IrCL1*_{Pp} was determined using a panel of selective small-molecule peptidase inhibitors listed in Table 1 together with their target peptidases. The *IrCL1*_{Pp} activity was completely blocked by peptidase inhibitors E-64 and Z-Phe-Phe-DMK, somewhat inhibited by CA-074 and unaffected by pepstatin, pefabloc and EDTA. This inhibition profile indicates that *IrCL1* has the ligand-binding characteristics typical of other cathepsins L.

3.8. Processing of macromolecular substrates by *IrCL1*

Haemoglobin and serum albumin represent the two major protein components of vertebrate blood (~80% w/w). After overnight

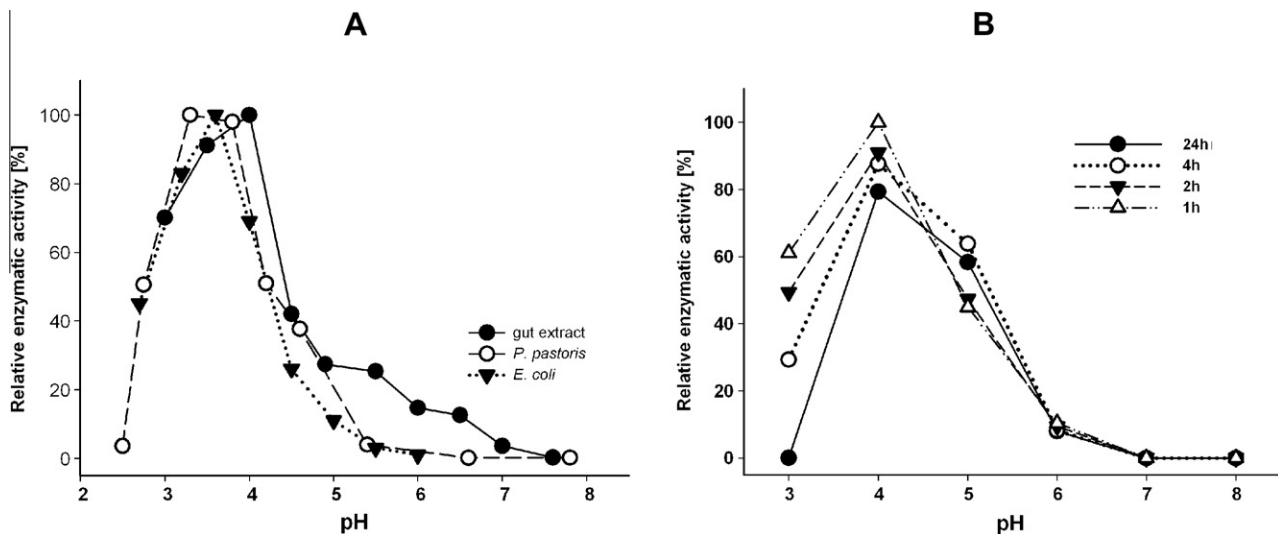


Fig. 6. Optimum pH and stability profiles of *Ixodes ricinus* cathepsin L (*IrCL1*). (A) Optimum pH of recombinant *IrCL1* expressed in *Escherichia coli* and *Pichia pastoris* was determined and compared with that of native *IrCL1* in tick gut homogenate. Activity was measured in a kinetic assay with the fluorogenic substrate Z-Phe-Arg-AMC (benzyloxycarbonyl-phenylalanylarginine-7-amido-4-methylcoumarin). Mean values (S.E. values were within 10%) are presented normalised to the maximum values (set as 100%). (B) The pH stability of recombinant *IrCL1* expressed in *P. pastoris* was examined by allowing the enzyme to stand for 1–24 h at room temperature. The activity of *IrCL1* was then measured using Z-Phe-Arg-AMC. Mean values (S.E. values were within 10%) are given normalised to the maximum value (set as 100%).

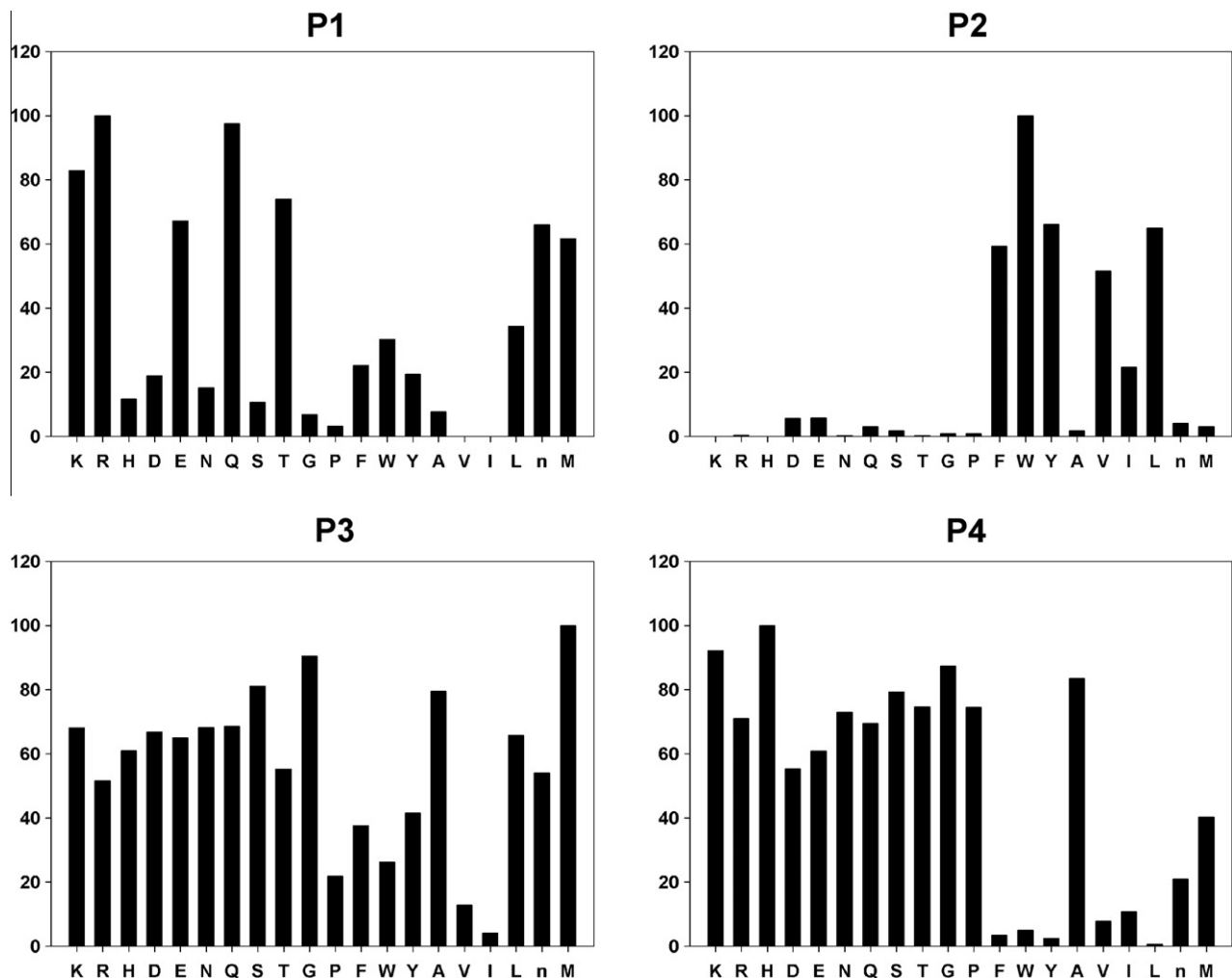


Fig. 7. P1–P4 specificity of *Ixodes ricinus* cathepsin L (*IrCL1*) determined by a positional scanning synthetic combinatorial library. *IrCL1* favours amino acids with polar side chains at P1, shows strong preferences for large hydrophobic residues at the P2 position and a higher level of promiscuity at the P3 and P4 positions. The Y axis represents activity related to the most preferred amino acid (100%). The X axis indicates the 20 amino acids held constant at each position, designated by the single-letter code (n, norleucine).

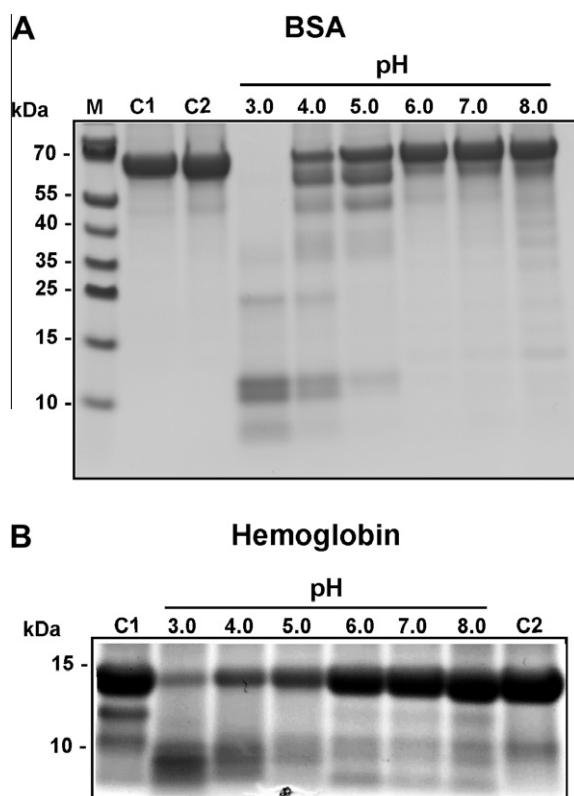


Fig. 8. Recombinant *Ixodes ricinus* cathepsin L (*IrCL1*) digests BSA and haemoglobin in vitro. (A) BSA (10 μ g) and (B) haemoglobin (10 μ g) were incubated overnight at room temperature with 15 ng of pure recombinant *IrCL1* expressed in *Pichia pastoris*. The protein digests were analysed by SDS–PAGE and then stained with Coomassie Blue. Controls with protein substrate alone (C1), and with a mixture of protein substrate, *IrCL1* and E-64 inhibitor (C2) were performed at pH 4.

incubation, both proteins were hydrolysed by *IrCL1*_{pp} and the mixture was subsequently analysed by SDS–PAGE (Fig. 8). The most effective hydrolysis of both protein substrates was observed at approximately pH 3.0 and efficiency of the fragmentation decreased with higher pH values. No hydrolytic activity was detected when the enzyme was inhibited with the Clan CA peptidase inhibitor, E64 (Fig. 8).

4. Discussion

A digestive system based on the proteolytic machinery consisting of cysteine clan CA, CD and aspartic A1 family peptidases is widespread in haematophagous invertebrates and stands in contrast to those systems of e.g. insects or vertebrates utilising serine peptidases (Sajid and McKerrow, 2002). A cascade or network involving cysteine and aspartic proteases has been proposed to catalyse haemoglobin degradation in many blood-feeding parasites such as platyhelminths (Caffrey et al., 2004; Delcroix et al., 2006), nematodes (Williamson et al., 2003) or *Plasmodium*, the malaria parasite (Rosenthal, 2004). Recently, we have demonstrated that the intestinal blood digestion in the semi-engorged *I. ricinus* is based on an analogous system of cysteine peptidases comprising cathepsins B, L and C, legumain (asparaginyl endopeptidase) and an aspartic peptidase cathepsin D arranged in the haemoglobinolytic cascade (Sojka et al., 2008; Horn et al., 2009). The gut-associated cathepsin L which, together with a cathepsin D aspartic peptidase, trigger the haemoglobin digestion in the gut of semi-engorged *I. ricinus* female are much less abundant than the downstream exo-/endopeptidases, cathepsins B and C (Horn et al., 2009; Franta et al., 2010). Thus cathepsins L and D represent

rational first-choice targets in an effort to efficiently interfere with blood digestion processes in ticks.

In the present study, we focused on finding the functional link between the *I. ricinus* cathepsin L gene and the cathepsin L activity in gut homogenates. Our previous screening of an *I. ricinus* gut-derived cDNA library resulted in isolation and cloning of an *I. ricinus* cathepsin L-related gene (*IrCL1*) (Sojka et al., 2008). A BLAST search for *IrCL1* related genes in the genome-wide database set for the closely related species, *I. scapularis* (<http://iscapularis.vectorbase.org>; December 2008 release), revealed a number of three cathepsin L paralogue genes designated as *IsCL1*, *IsCL2* and *IsCL3*. The multiple alignment shown in Supplementary Fig. S1 demonstrates that *IsCL1* is a clear orthologue of *IrCL1*, whereas the other two *I. scapularis* cathepsins L (*IsCL2* and *IsCL3*) as well as cathepsins L cloned from other tick species differ significantly from *IrCL1/IsCL1*, both in the sequence and glycosylation pattern (Supplementary Fig. S1). Our preliminary evolutionary analysis comprising cathepsins L from ticks and other selected organisms indicate a common ancestor gene within the Acari/Chelicerate group rather than relations between functional homologues described in the digestive systems of phylogenetically distant hematophagous parasites (data not shown). This further supports that adaptation of ticks to blood-feeding evolved independently as suggested earlier, based on the analysis of tick anti-haemostatic factors (Mans and Neitz, 2004).

The function of *IrCL1*-coded cathepsin L was assessed by the gene-specific RNAi knockdown which clearly demonstrated that *IrCL1* is the major enzyme form responsible for the cathepsin L activity in the gut homogenates from semi-engorged *I. ricinus* females (Horn et al., 2009). Also, the dynamics of the *IrCL1* mRNA and protein expression in tick gut homogenates during blood-feeding correspond with the cathepsin L enzyme activity profile measured in our previous work (Franta et al., 2010). Based on those profiles, *IrCL1* is maximally functional during the slow-feeding period of the tick between days 2 and 6 after attachment (Franta et al., 2010).

The recombinant *IrCL1* displays a narrow optimum pH at an acidic pH and low stability at a pH above 5. Both results agree with values measured in gut homogenates (Horn et al., 2009). As for other endopeptidases in the digestive gut machinery, e.g., *IrAE* and *IrCD* (Sojka et al., 2007; Horn et al., 2009), respectively, the restriction of *IrCL1* activity and stability to an acid pH may prevent undesired activity along the endolysosomal pathway and/or outside of the gut cells to protect the luminal food resource. Such protective mechanisms can be further fortified by the presence of cystatins in the gut lumen, as shown in the hard tick *Heamaphysalis longicornis* (Yamaji et al., 2010).

The substrate specificity profiling of *IrCL1*_{pp} shows that *IrCL1* displays substrate cleavage preferences similar to other Clan CA peptidases of cathepsin L-type of mammalian and parasitic origin (Choe et al., 2006; Stack et al., 2008). *IrCL1* shows the highest specificity at the P2 position, where just aromatic residues and large hydrophobic residues are preferred which by contrast are not allowed at the P4 position. This cleavage map of *IrCL1* mostly resembles that of cruzain except for the P3 position which in the tick enzyme is more promiscuous (Choe et al., 2006). The zero tolerance for Arg at the P2 position justifies the use of the Z-Arg-Arg-AMC substrate to clearly discern the activity of cathepsin B from that of cathepsin L in the gut homogenates (Franta et al., 2010). The substrate specificity of the non-primed subsites helps to explain the inhibitory specificity of *IrCL1*, which strongly interacts with substrate-analogue inhibitors leupetin (Ac-Leu-Leu-argininal) and Z-Phe-Phe-DMK (Table 1). In the former, Leu-Leu-argininal occupies the S3–S1 subsites and, in the latter, Phe-Phe occupies the S2–S1 subsites; all of these residues are preferred at the corresponding binding subsites.

Immunohistochemical localisation of IrCL1 in the vesicles of metabolically active gut cells displays a similar distribution compared with other haemoglobinolytic peptidases from *I. ricinus*, namely IrAE (Sojka et al., 2007) and IrCB (Franta et al., 2010), as well as cathepsin L from *R. microplus* (Renard et al., 2002). Tracing haemoglobin uptake by digestive cells of *R. microplus* suggested the presence of two separate endocytic pathways for the two most abundant host blood proteins, albumin and haemoglobin. Whereas albumin is absorbed by the fluid phase endocytosis and targeted to the small digestive vesicles, the potentially toxic haemoglobin is targeted to the larger vesicles via receptor-mediated endocytosis (Lara et al., 2005). We suppose that the tick heterophagy is a rather complex process which possibly shares several important features with mammalian endocytic mechanisms (for review see Doherty and McMahon, 2009). To this end, we hypothesise that the apical haemoglobinolytic enzymes such as IrCL1 or IrCD are preferentially targeted to the haemoglobin-containing endosomes. We assume that the IrCL1 pro-enzyme is activated at a low pH due to lysosomal acidification upon the fusion of primary lysosomes and endosomes (for review see Luzio et al., 2009). The hydrolysis of haemoglobin in the large acidic vacuoles may be further facilitated by its spontaneous denaturation that occurs below pH 4.5 (Gabay and Ginsburg, 1993). Recently, a similar functional study was performed for *Fasciola hepatica* cathepsin L1. The recombinant FheCL1 displayed a broad optimum pH (pH 5.5 to 7.0) in assays with peptidyl fluorescent substrate (Z-Phe-Arg-AMC) and ovalbumin indicating that FheCL1 functions both in the parasite gut and in the host tissues. However, haemoglobin could only be digested by FheCL1 below pH 4.5, which coincided with pH-induced dissociation of the haemoglobin tetramer (Lowther et al., 2009). The paradigm of possible synchronous action of cathepsin D and cathepsin L in the early stages of haemoglobin digestion has recently been demonstrated, whereby both enzymes were shown to generate haemoglobin-derived antimicrobial peptides in the *R. microplus* midgut (Cruz et al., 2010). Clearly, further co-localisation studies are required in order to specifically assign individual enzyme function(s).

Silencing of IrCL1 by RNAi impaired weight-gain of semi-engorged *I. ricinus* females fed for 6 days on guinea pigs. This result suggests that IrCL1 has a non-redundant role in the digestive machinery. Therefore, targeting this enzyme using specific immunotherapeutic antibodies provides a promising concept for the rational development of an anti-tick vaccine (Jongejan et al., 2007). Its effect may be augmented in combination with specific antibodies against the other promising vaccine candidates such as ferritin 2 (Hajdusek et al., 2010) or yet unexplored components of the tick digestive system.

Acknowledgements

This work was supported by Grant No. IAA 600960910 (to P.K. and M.M.) from the Grant Agency ASCR, Grant Nos. P207/10/2183 (to M.M. and P.K.) and No. P502/11/P682 (to D.S.) from the Grant Agency of the Czech Republic and by Research Center LC06009 (MSMT CR). Research at the Institute of Parasitology BC ASCR, Institute of Organic Chemistry and Biochemistry ASCR and Faculty of Sciences USB is covered by Research plans from MSMT CR, Nos. Z602205728, Z40550506 and MSM6007665801, respectively. J.D. was supported by a FP7 Marie Curie – International Re-integration Grant (248642) and by a Grant ME10011 (MSMT CR) awarded under the auspices of the American Science Information Center (AMVIS). C.R.C. was supported in part by the Sandler Foundation and Z.F. was the recipient of Sandler Foundation – supported research visit award. We thank Jan Erhart for the tick

collecting and rearing, and Jitka Konvickova for measuring of the cathepsin L activity in tick gut homogenates.

Appendix A. Supplementary data

Supplementary data associated with this article can be found, in the online version, at doi:10.1016/j.ijpara.2011.06.006.

References

- Anderson, J.M., Sonenshine, D.E., Valenzuela, J.G., 2008. Exploring the mialome of ticks: an annotated catalogue of midgut transcripts from the hard tick, *Dermacentor variabilis* (Acari: Ixodidae). BMC Genomics 9, 552.
- Aoyagi, T., Takeuchi, T., Matsuzaki, A., Kawamura, K., Kondo, S., 1969. Leupeptins, new protease inhibitors from *Actinomyces*. J. Antibiot. (Tokyo) 22, 283–286.
- Auld, D.S., 1988. Use of chelating agents to inhibit enzymes. Methods Enzymol. 158, 110–114.
- Barrett, A.J., Kembhavi, A.A., Brown, M.A., Kirschke, H., Knight, C.G., Tamai, M., Hanada, K., 1982. L-trans-Epoxy-succinyl-leucylamido(4-guanidino)butane (E-64) and its analogues as inhibitors of cysteine proteinases including cathepsins B, H and L. Biochem. J. 201, 189–198.
- Boldbaatar, D., Sikalizyo Sikasunge, C., Battsetseg, B., Xuan, X., Fujisaki, K., 2006. Molecular cloning and functional characterization of an aspartic protease from the hard tick *Haemaphysalis longicornis*. Insect Biochem. Mol. Biol. 36, 25–36.
- Buresova, V., Hajdusek, O., Franta, Z., Sojka, D., Kopacek, P., 2009. IrAM-An alpha2-macroglobulin from the hard tick *Ixodes ricinus*: characterization and function in phagocytosis of a potential pathogen *Chryseobacterium indologenes*. Dev. Comp. Immunol. 33, 489–498.
- Caffrey, C.R., Ruppel, A., 1997. Cathepsin B-like activity predominates over cathepsin L-like activity in adult *Schistosoma mansoni* and *S. japonicum*. Parasitol. Res. 83, 632–635.
- Caffrey, C.R., Salter, J.P., Lucas, K.D., Khiem, D., Hsieh, I., Lim, K.C., Ruppel, A., McKerrow, J.H., Sajid, M., 2002. SmCB2, a novel tegumental cathepsin B from adult *Schistosoma mansoni*. Mol. Biochem. Parasitol. 121, 49–61.
- Caffrey, C.R., McKerrow, J.H., Salter, J.P., Sajid, M., 2004. Blood 'n' guts: an update on schistosome digestive peptidases. Trends Parasitol. 20, 241–248.
- Choe, Y., Leonetti, F., Greenbaum, D.C., Lecaille, F., Bogyo, M., Bromme, D., Ellman, J.A., Craik, C.S., 2006. Substrate profiling of cysteine proteases using a combinatorial peptide library identifies functionally unique specificities. J. Biol. Chem. 281, 12824–12832.
- Coons, L.B., Rosell-Davis, R., Tarnowski, B.I., 1986. Blood meal digestion in ticks. In: Sauer, J.R., Hair, J.A. (Eds.), Morphology, Physiology, and Behavioural Biology of Ticks. Ellis Horwood Ltd., John Wiley & Sons, New York, pp. 248–279.
- Cruz, C.E., Fogaca, A.C., Nakayasu, E.S., Angeli, C.B., Belmonte, R., Almeida, I.C., Miranda, A., Miranda, M.T., Tanaka, A.S., Braz, G.R., Craik, C.S., Schneider, E., Caffrey, C.R., Daffre, S., 2010. Characterization of proteinases from the midgut of *Rhipicephalus (Boophilus) microplus* involved in the generation of antimicrobial peptides. Parasit. Vectors 3, 63.
- de la Fuente, J., Estrada-Pena, A., Venzal, J.M., Kocan, K.M., Sonenshine, D.E., 2008. Overview: ticks as vectors of pathogens that cause disease in humans and animals. Front. Biosci. 13, 6938–6946.
- Delcroix, M., Sajid, M., Caffrey, C.R., Lim, K.C., Dvorak, J., Hsieh, I., Bahgat, M., Dissous, C., McKerrow, J.H., 2006. A multienzyme network functions in intestinal protein digestion by a platyhelminth parasite. J. Biol. Chem. 281, 39316–39329.
- Doherty, G.J., McMahon, H.T., 2009. Mechanisms of endocytosis. Annu. Rev. Biochem. 78, 857–902.
- Franta, Z., Frantova, H., Konvickova, J., Horn, M., Sojka, D., Mares, M., Kopacek, P., 2010. Dynamics of digestive proteolytic system during blood feeding of the hard tick *Ixodes ricinus*. Parasit. Vectors 3, 119.
- Gabay, T., Ginsburg, H., 1993. Hemoglobin denaturation and iron release in acidified red blood cell lysate – a possible source of iron for intraerythrocytic malaria parasites. Exp. Parasitol. 77, 261–272.
- Greenbaum, D., Baruch, A., Hayrapetian, L., Darula, Z., Burlingame, A., Medzihradsky, K.F., Bogyo, M., 2002. Chemical approaches for functionally probing the proteome. Mol. Cell. Proteomics 1, 60–68.
- Hajdusek, O., Sojka, D., Kopacek, P., Buresova, V., Franta, Z., Sauman, I., Winzerling, J., Grubhoffer, L., 2009. Knockdown of proteins involved in iron metabolism limits tick reproduction and development. Proc. Natl Acad. Sci. USA 106, 1033–1038.
- Hajdusek, O., Almazan, C., Loosova, G., Villar, M., Canales, M., Grubhoffer, L., Kopacek, P., de la Fuente, J., 2010. Characterization of ferritin 2 for the control of tick infestations. Vaccine 28, 2993–2998.
- Horn, M., Nussbaumerova, M., Sanda, M., Kovarova, Z., Srba, J., Franta, Z., Sojka, D., Bogyo, M., Caffrey, C.R., Kopacek, P., Mares, M., 2009. Hemoglobin digestion in blood-feeding ticks: mapping a multiproteolytic pathway by functional proteomics. Chem. Biol. 16, 1053–1063.
- James, G.T., 1978. Inactivation of the protease inhibitor phenylmethylsulfonyl fluoride in buffers. Anal. Biochem. 86, 574–579.
- Jongejan, F., Nene, V., de la Fuente, J., Pain, A., Willadsen, P., 2007. Advances in the genomics of ticks and tick-borne pathogens. Trends Parasitol. 23, 391–396.
- Knight, C.G., Barrett, A.J., 1976. Interaction of human cathepsin D with the inhibitor pepstatin. Biochem. J. 155, 117–125.

- Kongsuwan, K., Josh, P., Zhu, Y., Pearson, R., Gough, J., Colgrave, M.L., 2010. Exploring the midgut proteome of partially fed female cattle tick (*Rhipicephalus (Boophilus) microplus*). *J. Insect Physiol.* 56, 212–226.
- Kopacek, P., Zdychova, J., Yoshiga, T., Weise, C., Rudenko, N., Law, J.H., 2003. Molecular cloning, expression and isolation of ferritins from two tick species – *Ornithodoros moubata* and *Ixodes ricinus*. *Insect Biochem. Mol. Biol.* 33, 103–113.
- Lara, F.A., Lins, U., Bechara, G.H., Oliveira, P.L., 2005. Tracing heme in a living cell: hemoglobin degradation and heme traffic in digest cells of the cattle tick *Boophilus microplus*. *J. Exp. Biol.* 208, 3093–3101.
- Levashina, E.A., Moita, L.F., Blandin, S., Vriend, G., Lagueux, M., Kafatos, F.C., 2001. Conserved role of a complement-like protein in phagocytosis revealed by dsRNA knockout in cultured cells of the mosquito, *Anopheles gambiae*. *Cell* 104, 709–718.
- Lowther, J., Robinson, M.W., Donnelly, S.M., Xu, W., Stack, C.M., Matthews, J.M., Dalton, J.P., 2009. The importance of pH in regulating the function of the *Fasciola hepatica* cathepsin L1 cysteine protease. *PLoS Negl. Trop. Dis.* 3, e369.
- Luzio, J.P., Parkinson, M.D., Gray, S.R., Bright, N.A., 2009. The delivery of endocytosed cargo to lysosomes. *Biochem. Soc. Trans.* 37, 1019–1021.
- Mans, B.J., Neitz, A.W., 2004. Adaptation of ticks to a blood-feeding environment: evolution from a functional perspective. *Insect Biochem. Mol. Biol.* 34, 1–17.
- Murata, M., Miyashita, S., Yokoo, C., Tamai, M., Hanada, K., Hatayama, K., Towatari, T., Nikawa, T., Katunuma, N., 1991. Novel epoxysuccinyl peptides. Selective inhibitors of cathepsin B, in vitro. *FEBS Lett.* 280, 307–310.
- Nijhof, A.M., Balk, J.A., Postigo, M., Jongejan, F., 2009. Selection of reference genes for quantitative RT-PCR studies in *Rhipicephalus (Boophilus) microplus* and *Rhipicephalus appendiculatus* ticks and determination of the expression profile of Bm86. *BMC Mol. Biol.* 10, 112.
- Nuttall, P.A., 1999. Pathogen–tick–host interactions: *Borrelia burgdorferi* and TBE virus. *Zentralbl. Bakteriol.* 289, 492–505.
- Pfaffl, M.W., 2001. A new mathematical model for relative quantification in real-time RT-PCR. *Nucleic Acids Res.* 29, e45.
- Renard, G., Garcia, J.F., Cardoso, F.C., Richter, M.F., Sakanari, J.A., Ozaki, L.S., Termignoni, C., Masuda, A., 2000. Cloning and functional expression of a *Boophilus microplus* cathepsin L-like enzyme. *Insect Biochem. Mol. Biol.* 30, 1017–1026.
- Renard, G., Lara, F.A., de Cardoso, F.C., Miguens, F.C., Dansa-Petretski, M., Termignoni, C., Masuda, A., 2002. Expression and immunolocalization of a *Boophilus microplus* cathepsin L-like enzyme. *Insect Mol. Biol.* 11, 325–328.
- Rosenthal, P.J., 2004. Cysteine proteases of malaria parasites. *Int. J. Parasitol.* 34, 1489–1499.
- Sajid, M., McKerrow, J.H., 2002. Cysteine proteases of parasitic organisms. *Mol. Biochem. Parasitol.* 120, 1–21.
- Sojka, D., Hajdusek, O., Dvorak, J., Sajid, M., Franta, Z., Schneider, E.L., Craik, C.S., Vancova, M., Buresova, V., Bogyo, M., Sexton, K.B., McKerrow, J.H., Caffrey, C.R., Kopacek, P., 2007. IrAE: an asparaginyl endopeptidase (legumain) in the gut of the hard tick *Ixodes ricinus*. *Int. J. Parasitol.* 37, 713–724.
- Sojka, D., Franta, Z., Horn, M., Hajdusek, O., Caffrey, C.R., Mares, M., Kopacek, P., 2008. Profiling of proteolytic enzymes in the gut of the tick *Ixodes ricinus* reveals an evolutionarily conserved network of aspartic and cysteine peptidases. *Parasit. Vectors* 1, 7.
- Sonenshine, D.E., 1991. *Biology of Ticks*. Oxford University Press, New York.
- Stack, C.M., Caffrey, C.R., Donnelly, S.M., Seshadri, A., Lowther, J., Tort, J.F., Collins, P.R., Robinson, M.W., Xu, W., McKerrow, J.H., Craik, C.S., Geiger, S.R., Marion, R., Brinen, L.S., Dalton, J.P., 2008. Structural and functional relationships in the virulence-associated cathepsin L proteases of the parasitic liver fluke, *Fasciola hepatica*. *J. Biol. Chem.* 283, 9896–9908.
- Tsuji, N., Miyoshi, T., Battsetseg, B., Matsuo, T., Xuan, X., Fujisaki, K., 2008. A cysteine protease is critical for *Babesia* spp. transmission in *Haemaphysalis* ticks. *PLoS Pathog.* 4, e1000062.
- Williamson, A.L., Brindley, P.J., Knox, D.P., Hotez, P.J., Loukas, A., 2003. Digestive proteases of blood-feeding nematodes. *Trends Parasitol.* 19, 417–423.
- Yamaji, K., Tsuji, N., Miyoshi, T., Islam, M.K., Hatta, T., Alim, M.A., Anisuzzaman, Takenaka, A., Fujisaki, K., 2009. Hemoglobinase activity of a cysteine protease from the ixodid tick *Haemaphysalis longicornis*. *Parasitol. Int.* 58, 232–237.
- Yamaji, K., Tsuji, N., Miyoshi, T., Hatta, T., Alim, M.A., Anisuzzaman, Kushibiki, S., Fujisaki, K., 2010. Hlcyst-1 and Hlcyst-2 are potential inhibitors of HICPL-A in the midgut of the ixodid tick *Haemaphysalis longicornis*. *J. Vet. Med. Sci.* 72, 599–604.